Minoru Seino was born in Niigata, Japan, in 1951. He received the B.E. and M.E. degrees in electrical engineering from Yokohama National University in 1975 and 1978, respectively.

He has been with Fujitsu Laboratories Ltd., Kawasaki, Japan, since 1978, where he has been engaged in the research and development of optical devices.

Mr. Seino is a member of the Institute of Electronics and Communication Engineers of Japan and the Japan Society of Applied Physics.

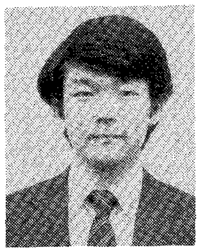

Ippei Sawaki was born in Kobe, Japan, in 1956. He received the B.S. and M.S. degrees in applied physics from the University of Tokyo, Tokyo, Japan in 1978 and 1980, respectively.

In 1980 he joined Fujitsu Laboratories Ltd., Kawasaki, Japan, and has been engaged in research on optical waveguide devices.

Mr. Sawaki is a member of the Institute of Electronics and Communication Engineers of Japan and the Japan Society of Applied Physics.

Multimode Deposited Silica Waveguide and Its Application to an Optical Branching Circuit

HIDEFUMI MORI AND NOBUO SHIMIZU

Abstract—**A fabrication procedure has been developed for multimode deposited silica waveguide (DS guide), consisting of uniform and thick glass layer formation for core and cladding, and amorphous Si mask film for reactive sputter etching. The embedded multimode DS guide with a square core cross section has a transmission loss of 1.3 dB/cm at 633 nm wavelength. Waveguide parameters, such as core dimension, refractive index, and index difference, are similar to those of a multimode silica fiber. A multimode optical branching circuit with eight output ports was demonstrated by the above fabrication procedure. Excess insertion loss was 2 dB.**

I. Introduction

MULTIMODE optical circuit components, such as an optical branch, a tap, a coupler, a filter, and a branching filter, will increase the usefulness of multimode optical fiber systems. In order to fabricate these components precisely and reproducibly, an ion exchange waveguide [1] and a polymer waveguide [2] have been demonstrated with a planar configuration by making use of a photolighographic process. To meet the low coupling loss requirement between these components and multimode fibers, it is preferable for the waveguides to have numerical aperture and core cross section similar to multimode fibers.

A new embedded silica waveguide, called deposited silica (DS) waveguide, has been demonstrated recently for single and multimode waveguide devices [3]. The DS guide is fabricated by planar processing of doped silica deposition followed by reactive sputter etching and has a rectangular cross-sectional core with a unity aspect ratio. It can have almost the same guide parameters as silica fibers because it is made of the same material. A single-mode directional coupler has been fabricated by utilizing this procedure [4].

For the multimode device application of this procedure, high rate and homogeneous glass deposition and sufficiently thick etching mask are essential. This paper reports results of studies on the DS guide fabrication method optimized for multimode waveguides, and a multimode optical branching circuit is demonstrated.

Manuscript received September 4, 1981.

The authors are with Musashino Electrical Communication Laboratory, Nippon Telegraph and Telephone Public Corporation, Tokyo, Japan.

II. DS Guide Fabrication

The DS guide fabrication method consists of two kinds of processes: silica deposition process to form core and cladding layers and core glass etching process according to a waveguide pattern. The glass particle deposition and glazing is similar to an optical fiber fabrication process, such as the VAD method [5]. This method enables making sufficiently thick glass layers. In the planar configuration presently considered, it is important to deposit glass particles uniformly in contrast with a silica fiber preform where radial uniformity is a main concern.

The waveguide pattern is defined by a reactive sputter etching process. This etching process is suitable for waveguide core fabrication with a rectangular cross section because of high etching selectivity between SiO_2 and a metal mask. A perpendicular core side wall can be obtained without undercutting. To make use of these preferable etching characteristics, sputtered amorphous Si was studied as etching mask material.

Fig. 1 shows the waveguide fabrication process.

(a) Doped silica glass particles are deposited as a core material on a fused quartz substrate.

(b) The glass particle layer is glazed transparent by exposing to high temperature.

(c) An amorphous Si film is deposited by RF bias sputtering

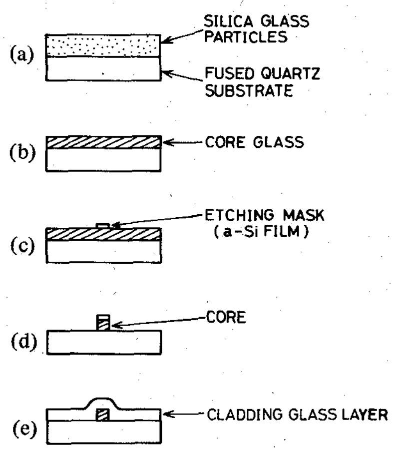

Fig. 1. DS guide fabrication process. (a) Silica glass particles deposition for a core layer on a fused quartz substrate. (b) Glazing to make the layer into a transparent core glass. (c) Etching mask formation. Amorphous Si film deposited by RF bias sputtering and fabricated to desired patterns by reactive sputter etching with $CBrF_3$ gas. (d) Core glass etching by reactive sputter etching with C_2F_6 and C_2H_4 gas mixture. (e) Silica glass particles deposition for cladding layer and glazing.

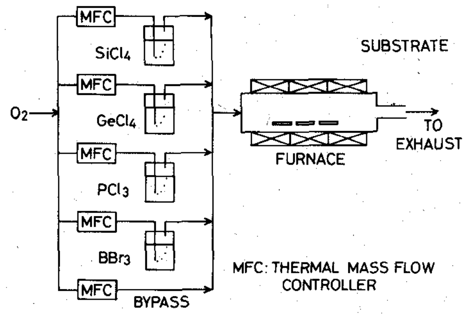

Fig. 2. Glass particle deposition apparatus diagram. A bypass path is provided for the carrier gas to adjust the total gas flow rate.

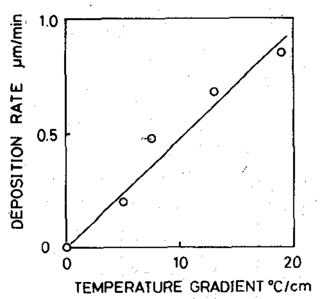

Fig. 3. Relation between deposition rate and temperature gradient. O_2 gas flow rates for $SiCl_4$, $GeCl_4$, and PCl_3 were 300, 250, and 300 ml/min, respectively.

for mask material. A desired mask pattern is formed by reactive sputter etching in $CBrF_3$ gas ambient.

(d) A rectangular core glass region is fabricated according to the waveguide pattern by reactive sputter etching with C_2F_6 and C_2H_4 gas mixture.

(e) Boron doped silica glass particles are then deposited and glazed to form a cladding layer. The glazing temperature is chosen to be lower than that for the core layer.

Each of the steps will be described in detail.

A. Glass Particle Deposition

Glass particles are synthesized from raw materials and deposited on a substrate in a furnace to make a uniform particle layer. Fig. 2 shows a schematic diagram of the deposition apparatus. Silicon tetrachloride $SiCl_4$ was used as the main raw material. Halides, such as $GeCl_4$, PCl_3, and BBr_3 were used as dopants which adjust the refractive index, softening temperature, and thermal expansion coefficient for the deposited glass. These materials were kept in saturaters, whose temperature was controlled to 20°C for $SiCl_4$ and PCl_3 and 10°C for $GeCl_4$. These materials were supplied on O_2 carrier gas into the furnace. Oxygen gas flow rate was controlled by a thermal mass flow controller. The furnace consisted of three zone heaters, which was able to adjust the temperature in each zone independently. This is because the reaction of the materials with O_2 gas depends on gas temperature, and they are fully reacted at 1200°C [6], while the particle deposition needs a temperature gradient, as will be mentioned later.

The silica glass particles' deposition rate depends on the raw material supply, furnace temperature, and total O^2 gas flow rate. Among them, the deposition rate depends most on the temperature gradient along the gas flow direction. No silica glass particles are deposited on a substrate without the temperature gradient, even if the furnace temperature is high enough to synthesize glass particles. Fig. 3 shows the relation between the deposition rate and the temperature gradient, when O_2 gas flow rates through $SiCl_4$, $GeCl_4$, and PCl_3 are 300, 250, and 300 ml/min, respectively, and bypass O_2 gas flow rate is 350 ml/min. The silica glass deposition rate, which is evaluated from the glass layer thickness obtained after glazing, increases linearly with increasing the temperature gradient. This means that a constant temperature gradient produces a constant thickness layer.

Fig. 4 shows the deposition rate distribution along the furnace, plotted for temperature gradient as a parameter. The deposition rate fluctuation is kept within 10 percent for the temperature gradient lower than 13°C/cm. The 13°C/cm temperature gradient was adopted in waveguide fabrication, at which the deposition rate was 0.7 μm/min. The important role of the temperature gradient in glass particle deposition is along the line with the results obtained in optical fiber fabrication [7], [8].

Refractive index of the deposited silica glass can be varied by adjusting O_2 gas flow rate through each dopant material saturater. The relations between refractive index and each dopant content have been studied in optical fiber fabrication [9]. The deposition condition for the core and cladding layer is shown in Table I.

B. Glazing

Deposited silica glass particles were made transparent by heating at above the glass softening temperature. Fig. 5 shows the slab waveguide loss dependence on the glazing temperature, where the core was prepared at the condition shown in Table I. The transmission loss was measured by moving an output prism coupler with matching oil between it and the waveguide at 633 nm wavelength. If the glazing temperature is higher than 1400°C, the waveguide loss approaches a constant value of 1 dB/cm. This fairly high loss is caused by scattering in the glass layer, as shown later.

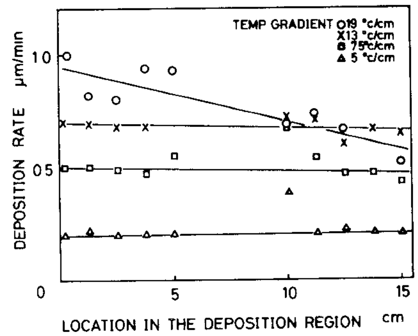

Fig. 4. Deposition rate distribution along the furnace axis. Deposition region corresponds to the center zone in the furnace.

TABLE I
GLASS DEPOSITION CONDITION

	Material	Saturater temperature (°C)	O_2 carrier gas flow rate (ml/min)	Total O_2 gas flow rate (ml/min)	Softing temperature (°C)	Relative refractive index difference from fused silica (%)
Core glass	$SiCl_4$	20	300			
	PCl_3	20	300	2200	1450	0.9
	$GeCl_4$	10	250			
Cladding glass	$SiCl_4$	20	300	2200	1100	- 0.1
	BBr_3	20	700			

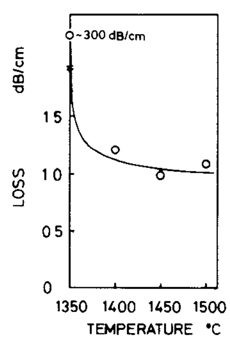

Fig. 5. Slab waveguide loss dependence on glazing temperature.

C. Etching Mask Formation

Cross-sectional dimensions for the multimode waveguide core is chosen to be 50 μm wide and 50 μm high according to that of a multimode optical fiber. This height requires deeper than 50 μm core glass etching. As the typical etching rate ratio SiO_2/metal is approximately 20 in reactive sputter etching with C_2F_6 and C_2H_4 gas mixture, the etching mask metal thickness has to be more than 2.5 μm. Metal films thicker than 1 μm prepared by sputtering or vacuum evaporation may often have a high internal stress and tend to peel off from substrates. To prepare a thick and stable etching mask, sputtered amorphous Si with low internal stress was studied.

A planar magnetron-type sputtering apparatus was used for amorphous Si. The RF bias power can be applied to a substrate holder, which can be heated up to 300°C. Internal stress in the film was calculated from the substrate curvature measured by a surface roughness tester.

Neither Ar sputtering pressure, ranging from 0.1 to 10 Pa, nor substrate temperature affected the a-Si compressive internal stress, which was on the order of 10^7 dyn/cm^2. Films with 10^7 dyn/cm^2 stress peel off from substrates, even if the thickness is less than 2 μm. In contrast, the RF bias power applied to substrate has a drastic influence on the a-Si internal stress. The result is shown in Fig. 6. The higher the RF bias power, the lower the internal stress, and the film stress turns from compressive to tensile at the 30 W RF bias power. Amorphous Si films, thicker than 5 μm, were prepared under the above condition and were stable for the etching process that follows.

Reactive sputter etching with $CBrF_3$ gas, which has been reported as the crystalline Si etching method without undercutting [10], was examined for patterning the a-Si film. Fig. 7 shows the etching characteristics for a-Si and AZ 1350J resist films. The etching rate of a-Si is approximately twice that of the resist for a high RF power. The resist surface was, however, roughened at the high RF power of 200 W. The resist

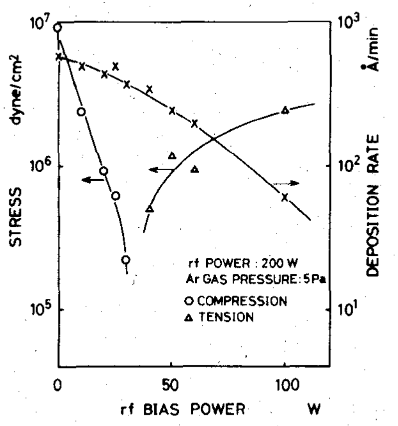

Fig. 6. Amorphous Si film internal stress as a function of RF bias power.

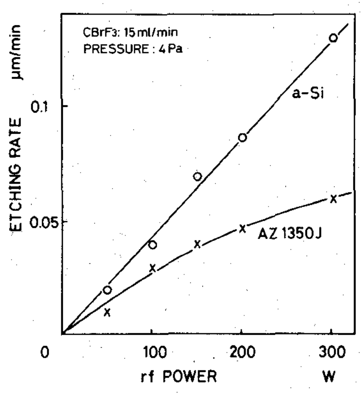

Fig. 7. Etching rate by reactive sputter etching with $CBrF_3$.

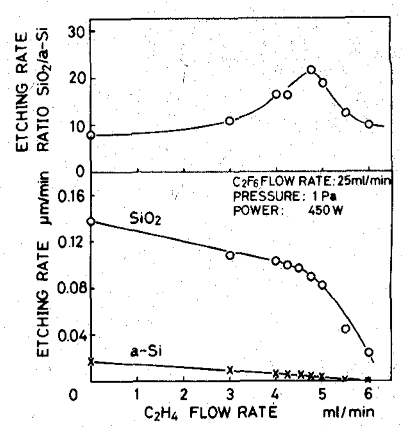

Fig. 8. Reactive sputter etching rate with C_2F_6 and C_2H_4 gas mixture.

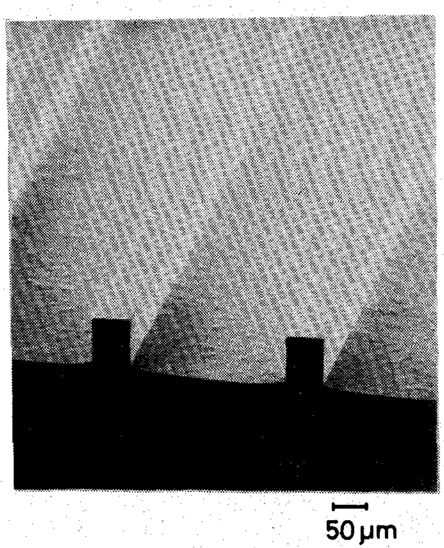

Fig. 9. SEM photograph of core ridge.

roughness causes the side wall roughness of the waveguide core. The side roughness can be kept less than 0.2 μm, if the applied RF power is lower than 100 W.

D. Core Width Definition

The core layer was etched by reactive sputter etching with C_2F_6 and C_2H_4 gas mixture. Fig. 8 shows etching characteristics for silica glass and a-Si. Etching rate ratio SiO_2/a-Si depends on the C_2H_4 gas flow rate. It reaches 21 at 4.7 ml/min C_2H_4 flow rate, 25 ml/min C_2F_6 flow rate, 1 Pa total gas pressure, and 450 W RF input power. Fig. 9 shows a scanning electron microscope (SEM) photograph of the multimode core ridge. It can be seen that the core side walls are almost vertical and the cross-sectional aspect ratio is unity.

E. Cladding Layer Preparation

A cladding glass layer was deposited on the same way as for the core glass, with the exception that BBr_3 was used as a dopant material instead of $GeCl_4$ and PCl_3, in order to obtain a lower refractive index and lower softening temperature glass. Cladding glass with a low softening temperature is essential to keep the core cross-sectional profile the same as etched in the previous procedure. Fig. 10 (a)-(c) shows the waveguide cross section deformation. Here, the softening temperature differences between core and cladding layer are 100, 200, and 350°C, respectively. The cladding layer with 300°C lower softening temperature than the core glass prevents the rectangular core shape from deformation.

III. Waveguide Properties

Optical properties of the multimode waveguide fabricated under the condition listed in Table I were examined. The refractive index differences between core and cladding glass and between cladding glass and fused quartz substrate were 0.9 percent and - 0.1 percent, respectively.

Transmission loss was measured as a function of waveguide core side wall roughness at 633 nm wavelength. The result is shown in Fig. 11, where the zero side wall roughness data were obtained from the waveguide with thermally deformed and smoothed core at a high glazing temperature. The transmission loss increases with increasing the core side wall roughness. The loss increase is less than 0.3 dB/cm, if the side wall roughness is less than 0.2 μm. The side wall roughness mainly comes from the resist pattern roughness caused in the a-Si mask patterning process. Less than 100 W RF input power in the reactive sputter etching process with $CBrF_3$ gas makes the core wall roughness less than 0.2 μm.

The DS guide absorption loss was lower than 0.1 dB/cm at 637 nm, measured by laser calorimetry [3]. According to the above-mentioned fact and the approximately 1 dB/cm slab waveguide total loss, it is concluded that the DS guide transmission loss is caused mainly by scattering in the core region.

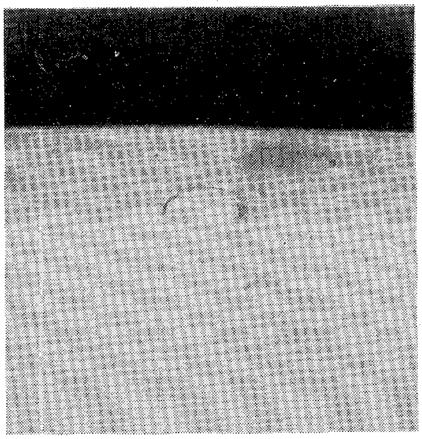

(a)

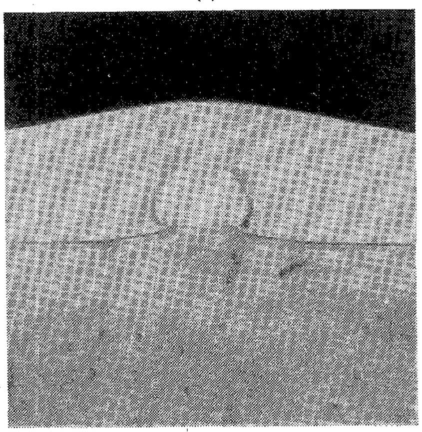

(b)

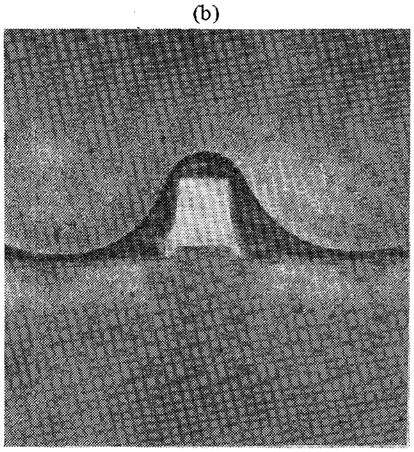

(c)

Fig. 10. Embedded waveguide cross section. Softening temperature differences between core and cladding glass are (a) 100°C, (b) 200°C, and (c) 350°C.

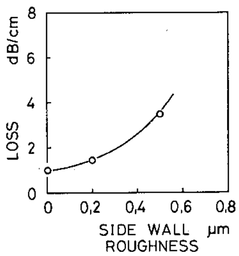

Fig. 11. Relation between loss and side wall roughness for multimode waveguide at 633 nm wavelength.

The coupling loss between the waveguide and graded index multimode fiber was 0.1 dB, where coupling was performed by a butt joint with matching oil.

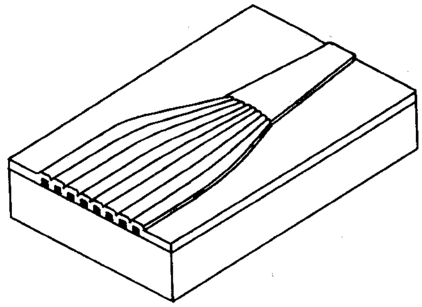

Fig. 12. Multimode optical branching circuit.

IV. Multimode Optical Power Branch

Multimode optical power branch, as shown in Fig. 12, was fabricated by the above-mentioned process. This circuit had an input port with 200 μm guide width and eight output ports with 50 μm guide width. The spacing between output branches was 200 μm. The waveguide curvature values at the branching curved section were 72, 100, 167, and 500 mm from the outside to the inside waveguide, respectively. The length of the curved waveguide region was 10 mm. Fig. 13 shows the output near-field patterns. It can be seen that the light power is divided almost equally. Fig. 14 shows circuit loss characteristics at 633 nm. Measurements were performed as follows. The 633 nm light from a He–Ne laser was first launched into a graded index multimode fiber with 50 μm core diameter. The multimode fiber was then butt jointed to the input port of the circuit using matching oil. The output from the branched waveguide was coupled into a step-index fiber with 80 μm core diameter. The loss characteristics were calculated from the light intensity differences between the input and output fibers. Average loss among output branches was 11 dB, loss deviation among them was ±1 dB, and the excess insertion loss was 2 dB. These characteristics were almost the same at 1.15 and 1.52 μm.

V. Summary

A deposited silica waveguide fabrication method was studied for embedded multimode waveguide. The results obtained are as follows.

1) Silica glass deposition rate is proportional to the temperature gradient along the furnace. Uniform thickness glass layers can be prepared by a constant temperature gradient. The deposition rate is 0.7 μm/min at the 13°C/cm temperature gradient.

2) The grazing temperature has no effect on waveguide loss, provided that it is higher than the glass softening temperature.

3) Thick etching mask for multimode waveguide fabrication can be prepared by RF bias sputtered a-Si films optimized for internal stress.

4) Multimode waveguide core with 50 μm rectangular cross section can be realized by reactive sputter etching processes.

5) Waveguide core dimensions are unchanged during the cladding layer formation at 300°C lower softening temperature than that for the core.

The DS guide, fabricated by this method, has a 1.3 dB/cm transmission loss at 633 nm, a 1.47 refractive index, and a 0.9 percent relative refractive index difference between core and fused quartz substrate. Core dimensions were almost the same as for a typical optical fiber. This gave rise to a low

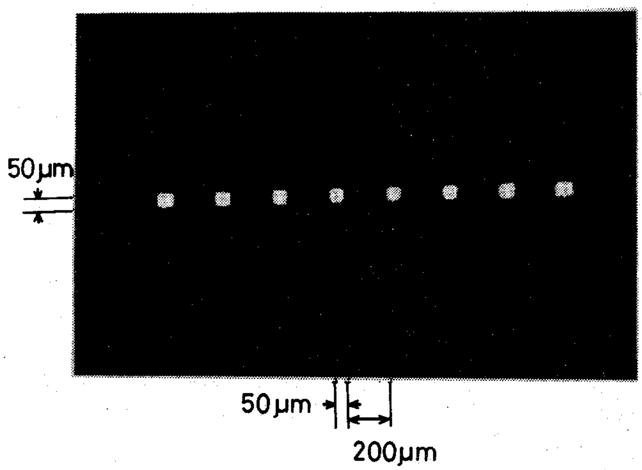

Fig. 13. Near-field patterns from multimode optical branching circuit at 633 nm wavelength.

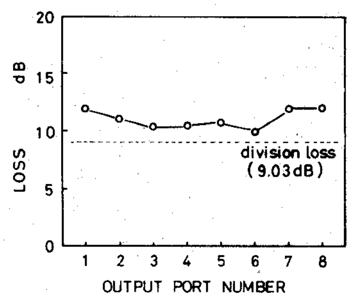

Fig. 14. Loss characteristics of multimode optical branching circuit at 633 nm wavelength.

coupling loss of 0.1 dB between DS guide and a multimode fiber. The DS guide is expected to fit into silica fiber transmission systems as one of their constituent components.

An optical branching circuit was prepared, using the DS guide, with 2 dB excess insertion loss and ±1 dB output power deviation at the wavelength range of 0.633-1.52 μm.

The DS guide fabrication method could be applicable to other multimode optical components, such as multiplexers, T and star couplers, and integrated optical circuits. Since the process is mainly based on photolithographic and etching processes, this method will provide an economic, reproducible, and mass productive method for making passive optical circuit components.

Acknowledgment

The authors wish to thank Dr. T. Kimura, Dr. M. Ikeda, and Dr. T. Izawa for helpful discussions.

References

[1] T. Izawa and H. Nakagome, "Optical waveguide formed by electrically induced migration of ions in glass plates," *Appl. Phys. Lett.*, vol. 21, pp. 584-586, Dec. 1972.

[2] T. Kurokawa, N. Takato, and Y. Katayama, "Polymer optical circuits for multimode optical fiber systems," *Appl. Opt.*, vol. 19, pp. 3124-3129, Sept. 1980.

[3] T. Izawa, H. Mori, Y. Murakami, and N. Shimizu, "Deposited silica waveguide for integrated optical circuits," *Appl. Phys. Lett.*, vol. 38, pp. 483-485, Apr. 1981.

[4] Y. Murakami, M. Ikeda, and T. Izawa, "Optical directional coupler using deposited silica waveguides (DS guide)," *IEEE J. Quantum Electron.*, vol. QE-17, pp. 982-987, June 1981.

[5] T. Izawa, S. Sudo, F. Hanawa, and S. Kobayashi, "Continuous fabrication of high-silica fiber preforms," *Elec. Commun. Lab. Tech. J.*, vol. 26, pp. 2531-2541, Sept. 1977.

[6] W. G. French, L. J. Pace, and V. A. Foertmeyer, "Chemical kinetics of the reactions of $SiCl_4$, $SiBr_4$, $GeCl_4$, $POCl_3$, and BCl_3 with oxygen," *J. Phys. Chem.*, vol. 82, pp. 2191-2194, 1978.

[7] P. G. Simpkins, S. Greenberg-Kosinski, and J. B. MacChesney, "Thermophoresis: The mass transfer mechanism in modified chemical vapor deposition," *J. Appl. Phys.*, vol. 50, pp. 5676-5681, Sept. 1979.

[8] K. L. Walker, F. T. Geyling, and S. R. Nagel, "Thermophoretic deposition of small particles in the modified chemical vapor deposition (MCVD) process," *J. Amer. Ceram. Soc.*, vol. 63, pp. 552-558, Sept.-Oct. 1980.

[9] B. G. Bagley, C. R. Kurkjian, J. W. Mitchell, G. E. Peterson, and A. R. Tynes, "Material, properties and choices," in *Optical Fiber Telecommunications*, S. E. Miller and A. G. Chynoweth, Eds. New York: Academic, 1979, pp. 167-231.

[10] S. Matsuo, "Selective etching of Si relative to SiO_2 without undercutting by $CBrF_3$ plasma," *Appl. Phys. Lett.*, vol. 36, pp. 768-770, May 1980.

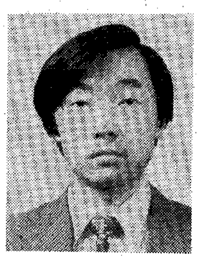

Hidefumi Mori was born in Tokyo, Japan, on February 15, 1948. He received the B.S. and M.S. degrees in instrumentation engineering from Keio University, Kanagawa, Japan, in 1971 and 1973, respectively.

He joined the Musashino Electrical Communication Laboratory, Nippon Telegraph and Telephone Public Corporation, Tokyo, Japan, in 1973, where he has been engaged in research on integrated optics and ultralow-loss fiber materials.

Mr. Mori is a member of the Institute of Electronics and Communication Engineers of Japan and the Japan Society of Applied Physics.

Nobuo Shimizu was born in Tokyo, Japan, on December 17, 1948. He received the B.S. degree from Nippon University, Japan, in 1971.

He joined the Musashino Electrical Communication Laboratory, Nippon Telegraph and Telephone Public Corporation, Tokyo, Japan, in 1967, where he worked on the development of Gunn diodes and traveling wave amplifier using GaAs and on the development of optical fiber connectors and fiber splicing technology. He is currently conducting research on integrated optics.

Mr. Shimizu is a member of the Institute of Electronics and Communication Engineers of Japan.